Preferential flow in the understory soil of *Hippophae rhamnoides* at different stump heights

Lu Liu[1†], Xiaoyu Liu[1†], Yunfeng Yao[1], Wei Qi[2] and Yuefeng Guo[1]*

[1]College of Desert Control Science and Engineering, Inner Mongolia Agricultural University, Hohhot, China, [2]Inner Mongolia Autonomous Region Water Conservancy Development Center, Hohhot, China

This study aimed to clarify the effects of stumping on preferential flow in the understory soils of *Hippophae rhamnoides* and to assess appropriate stumping height for optimization of preferential flow. Root properties, soil properties, and preferential flow for different *H. rhamnoides* stump heights (0, 10, 15, 20 cm, and no-stumping, labeled conditions S1, S2, S3, S4, and CK, respectively) were studied using *in situ* dye-tracing and laboratory analysis. The results showed that stumping significantly increased preferential flow development. This effect was maximized in condition S3, with dye-tracing coverage (DC) of 36.77%, maximum dye depth (MaxD) of 40.02 cm, uniform infiltration depth (Unifr) of 14.28 cm, preferential flow ratio (PF$_{fr}$) of 23.85%, and length index (LI) of 96.72%. In terms of root length density (RLD), root mass density (RMD), root surface area density (RSAD), soil water content (SWC), soil total porosity (TP), mean weight diameter (MWD), and soil organic matter (SOM), the conditions were ranked S3>S2>S1>S3>CK; for root average diameter (RAD), they were ranked S3<S2<S1<S4<CK. Structural equation modeling showed that DC was affected directly by TP, MWD, and SWC and indirectly by RAD, RLD, RMD, RSAD, and SOM, explaining up to 89.1% of the variance. Thus, stumping of *H. rhamnoides* affected soil properties through the mechanism of root development, thereby improving preferential flow development in the soil and soil infiltration. The optimal stump height was 15 cm. These findings are critical for vegetation recovery and for prevention and control of soil erosion in feldspathic sandstone areas.

KEYWORDS

stump height, preferential flow, vegetation recovery, compensatory growth, feldspathic sandstone

1 Introduction

The feldspathic sandstone region of Inner Mongolia is among the areas most severely affected by soil erosion on the Loess Plateau and worldwide. This region is a semiarid ecosystem. The proportion of semiarid ecosystems in China is about 22% (Guan and Hao, 2013). Feldspathic sandstones are under low diagenesis but become mud upon watering and turn into sand upon exposure to wind. This region has sparse natural vegetation and is undergoing severe erosion that is difficult to control. *Hippophae rhamnoides* is an important soil- and water-conserving plant in arid and semiarid areas. With good drought resistance and well-developed roots, it can propagate rapidly owing to its flourishing roots and strong tillering and germinating ability. It has excellent soil-water conservation abilities and is extremely dominant in the feldspathic sandstone areas of Inner Mongolia. In recent decades, ecosystem restoration has been undertaken in order to control land deterioration in the feldspathic sandstone region, which has demonstrated that planting *H. rhamnoides* can

optimally improve soil and water conservation (Zhang et al., 2017). However, an *H. rhamnoides* plantation that reaches 10 years of age will undergo massive decay and its productivity and soil and water conservation abilities will decrease (Yang et al., 2014; Cao et al., 2016). In contrast, shrubs appear to be able to compensate after stumping, enabling them to recover and grow, stimulate branch sprouting, and promote forest regeneration, thus improving soil and water conservation (Fang et al., 2006; Zhao et al., 2008). Stump height in particular is one of the controllable factors in this process (Giambalvo et al., 2011).

Soil moisture is a major factor restricting vegetation growth and distribution patterns in arid and semiarid areas. Rain infiltration is an important source of soil moisture and determines the level of impoundment and surface runoff in soils (Wu et al., 2017; Sun et al., 2018). Preferential flow, as a major form of soil moisture infiltration, refers to the process by which soil water passes through the soil matrix and preferentially moves toward an underground water source (Zhang et al., 2016). Preferential flow is closely related to ecosystem stability and plays a critical role in hydrological processes (Shao et al., 2015; Khan et al., 2016). Preferential flow can affect infiltration processes, decrease runoff and soil erosion, and increase moisture around a root zone, thus significantly affecting deterioration in arid areas (Wang et al., 2020; Zhu et al., 2020). Although preferential flow routes only account for 0.1%–5% of soil volume, the preferential flow infiltration speed is 2–10 times the soil matrix infiltration speed and is very stable (Jarvis, 2007; Zhan et al., 2019). Thus, evaluation of the preferential infiltration process is critical, as this process is very important in the ecological functions of soil (Jiang et al., 2019).

Currently, the main methods employed in preferential flow research include dye tracing, indoor soil column experiments, computed tomography, magnetic resonance imaging, and underground radar probing. Among these, the dye-tracing method in particular allows for direct observation of the number and morphology of large soil pores. Thus, this easy-to-use and low-cost method is widely applied (Weiler and Fluhler, 2004; Zhang and Yuan, 2019). Time–space changes in soil preferential flow are mainly affected by complex interactions between topographic properties, soil properties, vegetation types, and animal activities (Liu and Lin, 2015; Maier et al., 2020; Liu et al., 2021). A highly heterogeneous soil configuration greatly affects the generation of preferential flow (van Schaik, 2009; Wang et al., 2018). The presence of gravel in soils affects the number of large pores, while the density and volume of valid pores affect the occurrence of preferential flow. The distribution of soil macropores is heavily affected by soil bulk density and organic matter content (Mei et al., 2018). Recent research (Luo Z. et al., 2019; Guo et al., 2019) has focused on the effects of plant roots on preferential flow. The metabolic activities of roots, as well as the presence of rotten roots, generate root pores, thereby forming preferential flow routes. In the Loess Plateau of North China, root length density and volume density are significantly increased by plant recovery; plant patches thereby intensify spatial variation in moisture infiltration and preferential flow (Wang et al., 2020).

The formation of macroporous channels in plant roots plays a key role in infiltration in arid and semiarid areas (Cui et al., 2019; Wu et al., 2020). Stumping stimulates root growth and intensifies the metabolic ability of roots, thereby affecting the infiltration processes

of soils (Wang et al., 2020; Liu et al., 2022). However, existing relevant research is almost entirely restricted to studies of stumping or sprouting, especially the relationships of stubble sprouting and branch number with biomass increment (Langworthy et al., 2019; Yang et al., 2020). There is no existing research on the influence of stump height on sprouting capacity, nor on the relevant systems. Moreover, it is unknown how stump height affects soil properties and root properties in feldspathic sandstone areas, and how root and soil properties in turn affect soil preferential flow behaviors. For this reason, the present study focused on decaying *H. rhamnoides* in the feldspathic sandstone region of Inner Mongolia. In particular, the effects of stump height on root and soil properties and the direct and indirect effects of root and soil properties on preferential flow were explored. The aim of the study was to uncover the ecological mechanism of the rapid reproduction of *H. rhamnoides* after stumping to enable full utilization of the soil and water conservation functions of *H. rhamnoides*. The findings provide theoretic basis for the understanding of vegetation recovery, soil water, and efficient fertilizer use, and for prevention and control of soil-water loss in this region.

The aims of this study were (1) to evaluate the effects of stump height on root and understory soil properties in *H. rhamnoides* forests, (2) to determine the degree of preferential flow development at different stump heights using the dye-tracing method, and (3) to assess the mechanism underlying the effect of stump height on soil preferential flow and identify the optimal stump height.

2 Materials and methods

2.1 Experimental sites

The study area belongs to the Inner Mongolia feldspathic sandstone region; the specific location was the demonstration plot for soil-water conservation science in the Jungar Banner Village of Nuanshui, Ordos, Inner Mongolia. This watershed (39°42′N—39°50′N, 110°25′E–110°48′E, 96 km²) has fluctuating terrains and numerous gullies, with fluctuating girders, but undergoes strong soil erosion and severe soil-water loss. With an average altitude of 800–1,590 m, this area has a typical moderate-temperature semiarid continental monsoon climate, with an average sunshine duration of 2,900–3,100 h and a frost-free period of 148 days. The average precipitation is approximately 400 mm, average evaporation is 2,093 mm, and the annual average temperature is 6.2°C–8.7°C. The winds are strong and persistent in the spring, with an annual wind speed of 3.2 m/s, a maximum speed of 32 m/s, and 10–30 days of strong wind. The dominant soil type is loessial soil, which is accompanied by chestnut and sand soils. This watershed is planted mainly with artificial vegetation. The major afforestation species include *H. rhamnoides*, *Pinus tabuliformis Carr.*, *Caragana korshinskii Kom.*, *Medicago sativa Linn.*, and *Prunus sibirica Lam.*

2.2 Experimental design

Within the soil-water conservation science demonstration plot a wintering *H. rhamnoides* plantation was selected as the experimental

site, under consistent site conditions and forest conditions, situated on a northwest slope face with a slope of 4°. Trees were planted with row spacing of 2 m × 4 m on the same slope face. Trees were stumped in early March of 2020 at stump heights of 0, 10, 15, and 20 cm above the ground; these heights were designated as treatments S1, S2, S3, and S4, respectively. A plantation site without stumping was designated as a control (CK). Each space within a site was 50 m × 50 m, and each treatment was conducted in triplicate. For this purpose, three trees were selected at each site. Stumping was conducted using electric saws and pruning shears, which ensured that the incisions were flat and smooth, without burrs. The stumping mode was complete stumping. To reduce moisture dissipation, the trees were painted after stumping (Liu et al., 2023a). In September 2022, dye-tracing experiments were conducted in all plots. Subsequently, five typical root groups from each site, exposed to consistent and representative conditions, were selected for collection and analysis of roots and soils (Figure 1).

2.2.1 Dye-tracing experiments

A total of 25 dye-tracing experiments (5 treatments × 5 repetitions) were conducted, covering each of the different stump heights. The soil humus layer was not destroyed, but ground litter and large stones were cleared to expose the ground surface. Rectangular metal frames (100 cm length × 50 cm width × 30 cm height) were placed vertically into the soil at a depth of 15 cm, and the areas of contact between the metal frames and soil were smeared with an appropriate amount of Vaseline to prevent moisture infiltration. The dye-tracing experiments were conducted when no rainfall had occurred on the test day, nor one day before or one day after the experiments. The tracer was 4 g L^{-1} brilliant blue. Each sampling site was irrigated with 7.5 L of the dye solution (Song et al., 2019). Brilliant blue is often used as a tracer because of its high fluidity and visibility (Luo Z. et al., 2019). The brilliant blue solution was evenly irrigated onto the soil surface within the metal frames at a rate of 15 mm/h (a simulated rainfall intensity of 15 mm h^{-1}, equivalent to local moderate precipitation) (Liang et al., 2020). The sprayed areas were then covered with black plastic to prevent evaporation, precipitation, and other external conditions from interfering with the experiments. Subsequently, 24 h after the end of the dye-tracing experiments, the metal frames were removed without destroying the dyed soils. In the middle of the irrigated area, a soil section (100 cm width × 50 cm depth) was excavated. Each layer was 10 cm of the vertical section. The deepest excavation depth was determined by the dyed depth. After each section was excavated, it was appropriately trimmed. The width and depth of the dyed area were then measured using a straight scale. The soil sections were photographed using an AF-SD5600 digital camera (Nikon, Tokyo, Japan); these images formed the basis for subsequent trace analysis.

2.2.2 Measurement of root parameters

Sections were excavated on each sampling site. In the 0–50 cm layer, the roots were sampled at a layer depth of 10 cm using a root drill (d = 70 mm, h = 150 mm). Rootless soils were then shaken off and soils containing roots were placed into valve bags. A total of 375 root samples were collected (5 treatments × 3 repetitions × 5 plants × 5 layers). The roots were taken back to the laboratory, screened using 0.25 mm sieves, and washed with deionized water.

Surface water was removed from the roots using nonwoven fabrics. The roots were scanned using a 11000XL scanner (Epson, Tokyo, Japan). The average diameter (RAD), length, and surface morphology were measured using a WinRHIZO Pro 2012b (Regent Instruments Inc., Quebec City, Canada). The roots were then dried in an oven at 60°C for 48 h, their weight was monitored, and the dry weight was recorded at constant weight (Liu et al., 2023b). Finally, root length density (RLD, cm cm^{-3}), root mass density (RMD, mg cm^3), and root surface area density (RSAD, cm^2 cm^{-3}) were calculated. RLD refers to the ratio of the root length to soil volume; RMD is the ratio of root dry mass to soil volume; and RSAD refers to the ratio of root surface area to soil volume (Cao et al., 2021).

2.2.3 Measurement of soil properties

Soil sampling and root sampling were performed synchronously. In the 0–50 cm soil layer, soils were sampled at a layer depth of 10 cm using standard 100 cm^3 cylinders (d = 50.46 mm, h = 50 mm) and large aluminum boxes. Soil total porosity (TP, %), soil organic matter (SOM, g kg^{-1}), soil water content (SWC, %), and soil aggregates were then measured. SOM was monitored using the dichromate titration-external heating method. SWC was determined by drying the samples in an oven at 105°C for 24 h until a constant weight was reached. The stability of soil aggregates was measured using the rapid wetting method (Hao H. X. et al., 2020) and mean weight diameter (MWD, mm), which was computed as follows:

$$MWD = \frac{\sum_{i=1}^{i=6} M_i \times D_i}{\sum_{i=1}^{i=6} M_i},\qquad(1)$$

where M_i is the mass at each particle size (g) and D_i is the average diameter of each particle size (mm). (D_1 is 3.500 mm, and D_6 is 0.053 mm).

2.2.4 Quantification of preferential flow

Dye-tracing coverage (DC, %) reflects the proportion of dyed area in the total soil section (Flury et al., 1994):

$$DC = \left(\frac{D}{(D + ND)}\right) \times 100,\qquad(2)$$

where D is the total dyed area in the soil section (cm^2) and ND is the undyed area of the soil section (cm^2).

Preferential flow fraction (PF_{fr}, %) refers to the total percentage penetration passing through preferential flow channels (van Schaik, 2009), and is calculated as follows:

$$PF_{fr} = \left(1 - \frac{Unifr \times W}{TSA}\right) \times 100,\qquad(3)$$

where $Unifr$ is the uniform flow fraction of the matrix (cm), W is the horizontal width of the soil section (here 100 cm), and TSA is the total dyed area of the soil section (cm^2).

Length index (LI, %) refers to the absolute difference between DC and the vertical section depth (Tobella et al., 2014):

$$LI = \sum_{i=1}^{n} |DC_{i+1} - DC_i|,\qquad(4)$$

FIGURE 1
Scheme of the dye-tracing experiment and image analysis processes. **(A)** Vertical section diagram. **(B)** Cutting and noise reduction in Photoshop. **(C)** Extraction of the dyed regions.
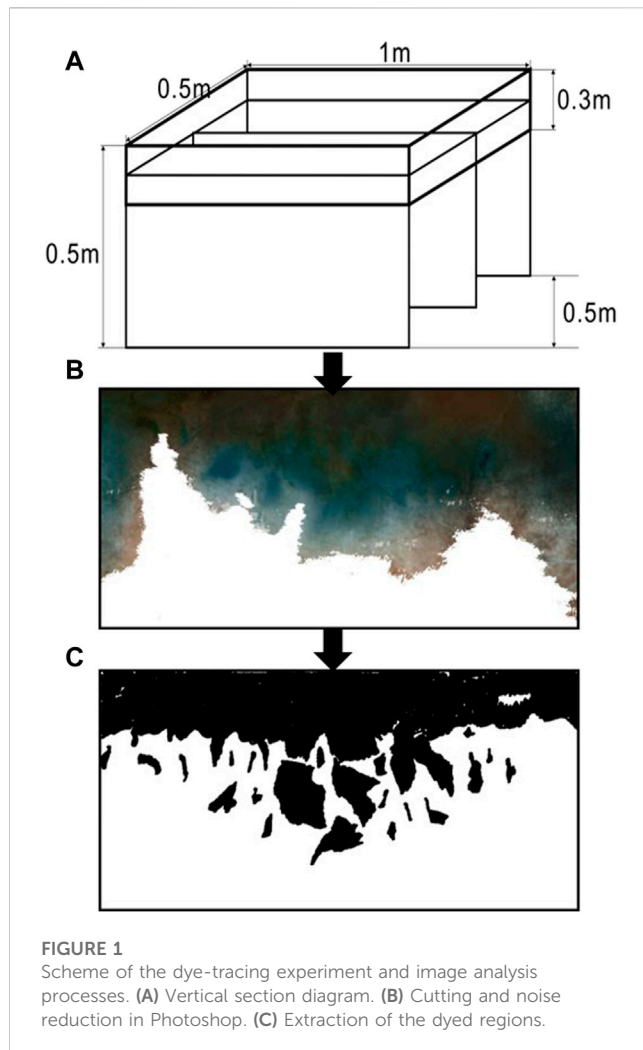
where DC_i and DC_{i+1} represent the coverage area of dye in layers i and $i+1$, respectively, and n is the number of vertical soil layers in the soil section.

MaxD is the maximum depth in the dyed area (cm).

2.3 Statistical analysis

The dye-tracing images were geometrically calibrated and trimmed using Adobe Photoshop CS5. Subsequently, the pictures were reclassified, thresholds were set, and they were binarized and pixel-extracted in Matlab 2015. The differences in root properties, soil properties, and preferential flow for different stump heights were evaluated via one-factor analysis of variance (ANOVA). Significance tests were conducted using Fisher's least significant difference (LSD) at a significance level of $p < 0.05$. The spatial distributions of preferential flow for different stump heights were plotted using Surfer version 14. The relationships between preferential flow and soil properties or root properties were determined via Pearson's correlation analysis. Structural equation models (SEMs) were constructed and the direct and indirect effects of root properties and soil properties on soil preferential flow were assessed using Amos21. Statistical analysis was performed using IBM SPSS Statistics for Windows, version 24.0. Final plots were created using Origin 2021.

3 Results

3.1 Preferential flow with different stump heights

Analysis of the soil preferential flow index for different stump heights showed that higher indices were achieved after stumping compared to without stumping. Preferential flow indices for S2 and S3 differed significantly from that of CK ($p < 0.05$). In terms of DC, MaxD, Unifr, and LI, the stump height conditions were ranked as follows: S3>S2>S1>S4>CK; in terms of PF$_{fr}$, the ranking was S3<S2<S1<S4<CK (Table 1).

The dyed areas in conditions S1, S2, S3, and S4 were concentrated at 0–30 cm depth. The dyed area for CK was shallower and concentrated at 0–20 cm depth, with dye coverage decreasing significantly beyond 20 cm. In condition S1, the dyed area ratio gradually increased between 0 and 3 cm depth, essentially stabilized after reaching its peak, and then started to decrease until a depth of 10 cm. The dyed area ratio began to decrease significantly beyond a depth of 25 cm, with an overall dyed depth of up to 26–32 cm (Figures 2A, F). In S2, the dyed area ratio gradually increased at a depth of 0–3 cm, essentially stabilized after reaching its peak, and then started to decrease until a depth of 13 cm. The dyed area ratio started to significantly decrease beyond a depth of 36 cm, with a dyed area ratio of approximately 25% at a depth of 28 cm and an overall dye depth of up to 32–38 cm (Figures 2B, G). In S3, the dyed area ratio gradually increased at a depth of 0–3 cm, essentially stabilized after reaching its peak, and then began

TABLE 1 preferential flow characteristics.

Treatment	DC (%)	MaxD (cm)	Unifr (cm)	PF$_{fr}$ (%)	LI (%)
S1	26.02 ± 2.27b	31.67 ± 1.74b	8.51 ± 1.56bc	34.67 ± 3.40bc	87.50 ± 5.12a
S2	29.64 ± 2.08b	38.33 ± 3.69a	10.33 ± 2.04b	30.30 ± 2.66c	94.97 ± 1.32a
S3	36.77 ± 2.26a	40.02 ± 2.69a	14.28 ± 1.93a	23.85 ± 4.12d	96.72 ± 1.94b
S4	19.79 ± 1.21c	31.66 ± 1.94b	6.33 ± 1.48cd	36.03 ± 1.22b	65.81 ± 4.20c
CK	14.74 ± 2.76d	30.13 ± 2.34b	3.66 ± 0.83d	50.34 ± 2.49a	54.11 ± 2.61d

Note: Values are mean ± SD. DC, dye-tracing coverage; MaxD, maximum dye depth, Unifr, uniform infiltration depth; PF$_{fr}$, preferential flow ratio; LI, length index. Significant differences are indicated by different lowercase letters at $p < 0.05$.
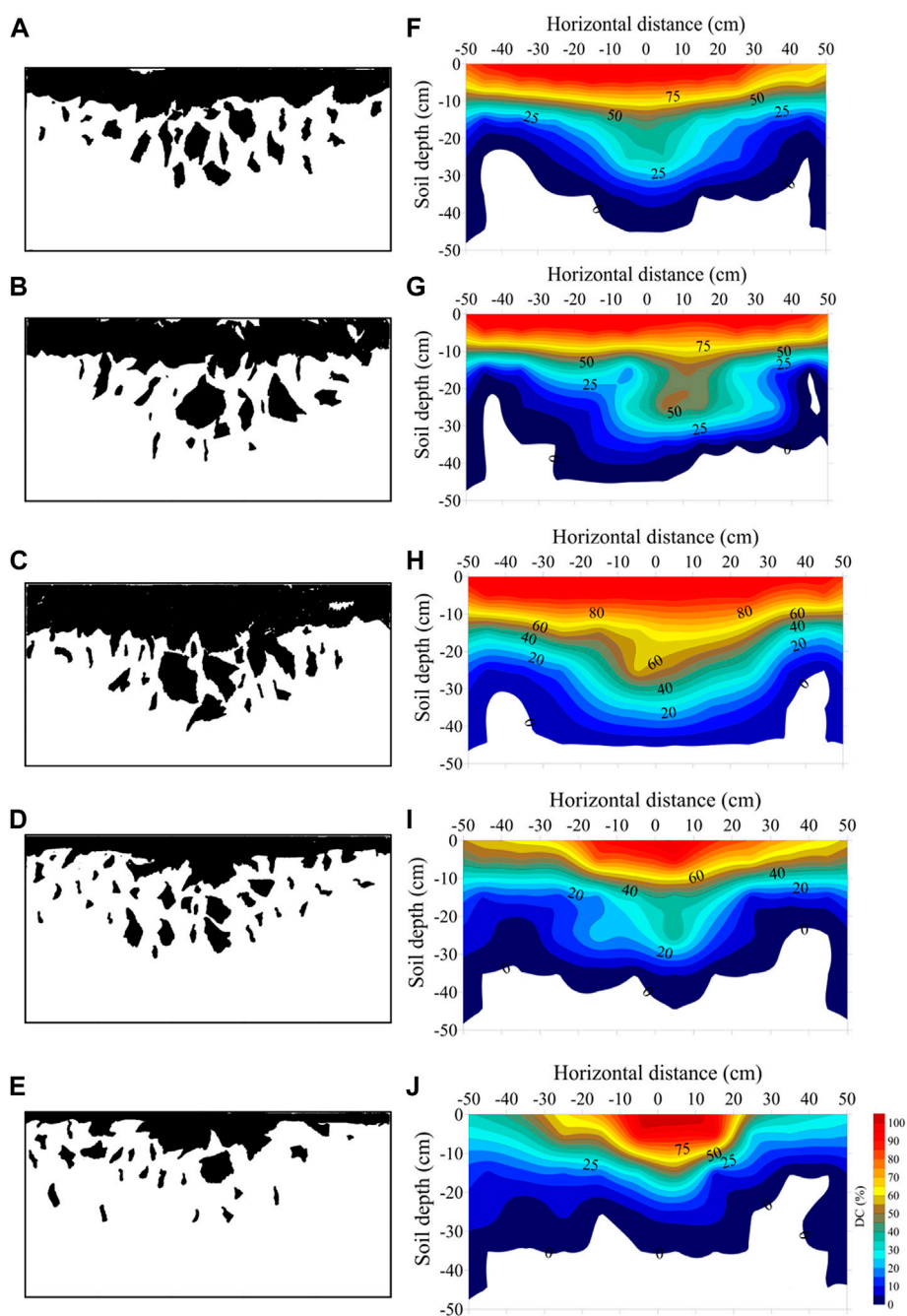
FIGURE 2
Binarized images and spatial distributions of dyed proportion for different stump heights. **(A–E)** Binarized images for stump heights of 0, 10, 15, and 20 cm, and no-stumping, respectively. **(F–J)** Spatial distributions of dyed area proportion for stump heights of 0, 10, 15, and 20 cm, and no-stumping, respectively.

to decrease until a depth of 15 cm. The rate of decrease in the dyed area ratio increased at a depth of 38 cm, with a dyed area ratio of 25% at dyed depths below 30 cm and an overall dyed depth of up to 36–40 cm (Figures 2C, H). In S4, the dyed area ratio gradually increased at a depth of 0–3 cm, essentially stabilized after reaching the peak, and then started to decrease until a depth of 10 cm. The rate of decrease in the dyed area ratio increased at a depth of 20 cm, with a dyed area ratio of 25% at dye depths above 20 cm and an overall dye depth up to 25–31 cm (Figures 2D, I). Finally, in condition CK, the dyed area ratio gradually increased at a depth of 0–3 cm, essentially stabilized after reaching its peak, and then started to decrease at a depth of 9 cm. The dyed area ratio was 25% at a dye depth of 10 cm, with an overall dye depth of up to 18–23 cm (Figures 2E, J).

FIGURE 3
Changes in root traits with soil depth for different stump heights. **(A)** Average root diameter, **(B)** root length density, **(C)** root mass density, and **(D)** root surface area density.
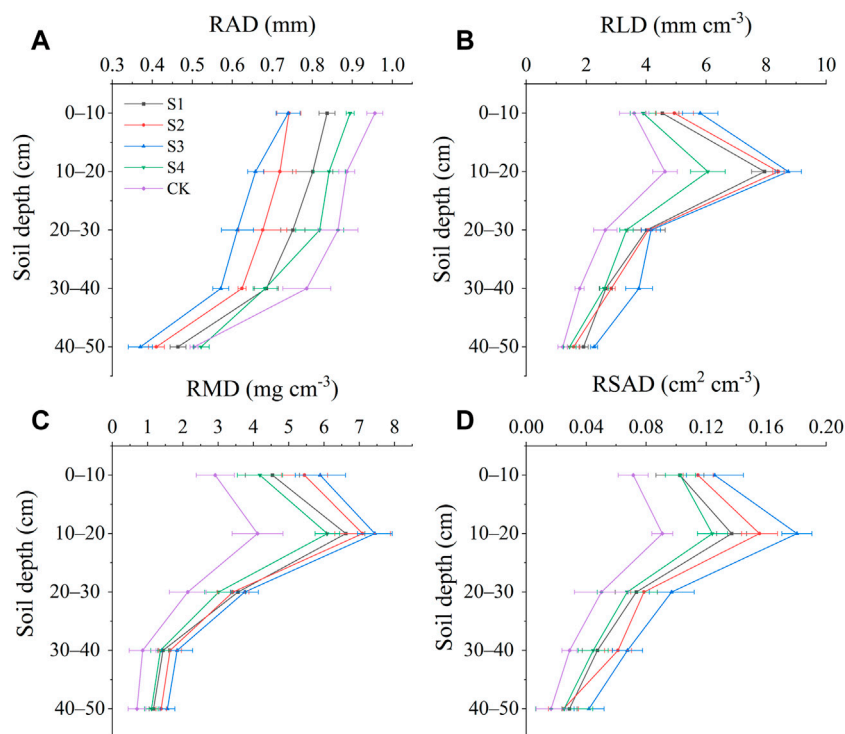
3.2 Root traits for different stump heights

Root properties differed among the different stump heights (Figure 3). RAD significantly decreased with increasing soil depth and differed significantly by stump height. The conditions ranked as follows in terms of RAD: CK>S4>S3>S2>S1. The RAD range was 0.37–0.74 mm in condition S3 and 0.50–0.96 mm in CK (Figure 3A). Unlike RAD, RLD, RMD, and RSAD all initially increased and then decreased with increasing soil depth. RLD, RMD, and RSAD all reached their maximum at a depth of 10–20 cm regardless of stump height, and all differed significantly by stump height. The differences among stump heights gradually decreased at a depth of 30–50 cm. In terms of RLD, RMD, and RSAD, the stump height conditions ranked as follows: S3>S2>S1>S4>CK (Figures 3B–D).

3.3 Soil properties with different stump heights

Analysis of the understory soil properties associated with different stump heights showed that, for each stump height, SWC first increased at a soil depth of 0–20 cm, and then decreased at a depth of 20–50 cm, peaking at a depth of 10–20 cm. The water content at a depth of 10–20 cm was 1.30 times greater in condition S3 (11.11%) than in CK (8.54%)

(Figure 4A). The differences among the stump height conditions in terms of SWC narrowed at a depth of 40–50 cm, consistent with the distributive laws of RLD, RMD, and RSAD among soil layers (Figures 3B–D). The distributive laws of TP, MWD, and SOM among different layers were inconsistent with the distribution of water content; TP, MWD, and SOM all decreased with increasing soil depth. The differences by stump height were larger for SOM compared to the differences in TP and MWD. SWC, TP, MWD, and SOM were all greater in each of the stump conditions compared to the CK condition, and the conditions ranked as follows: S3>S2>S1>S4>CK. SWC, TP, MWD, and SOM for S3 were 1.22, 1.16, 1.17, and 2.07 times greater than the values for CK, respectively (Figure 4).

3.4 Factors influencing soil preferential flow

Pearson correlation analysis of root and soil properties in terms of their association with proportion of soil-dyed area (Figure 5) showed that RAD was very strongly negatively correlated with DC ($p < 0.001$). RLD, SWC, TP, MWD, and SOM were all very strongly positively correlated with DC ($p < 0.001$). RSAD was not correlated with DC ($p > 0.05$). RAD was very strongly negatively correlated with RLD ($p < 0.001$). RMD was positively correlated with RLD and RSAD ($p < 0.05$). TP and SWC were strongly positively correlated with MWD and SOM ($p < 0.01$). SWC, TP, MWD, and SOM were all strongly
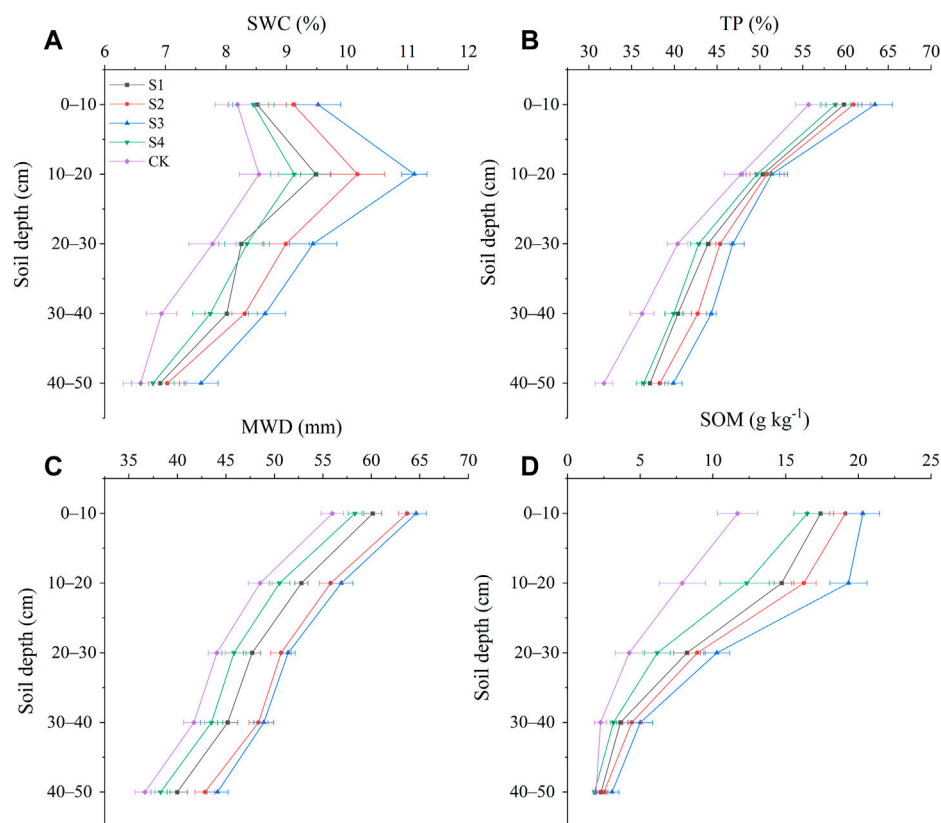
FIGURE 4
Changes in soil properties with soil depth for different stump heights. **(A)** Soil water content, **(B)** soil porosity, **(C)** mean weight diameter, and **(D)** soil organic matter.

negatively correlated with RAD ($p < 0.01$) and strongly positively correlated with RLD ($p < 0.01$). Finally, SWC was positively correlated with RMD and RSAD ($p < 0.05$).

Structural equation modeling showed that root and soil properties significantly affected the dyed area ratio of soil preferential flow and was further used to visualize the interactions, direct effects, and indirect effects of various variables. TP, MWD, and SWC explained 89.1% of the soil dyed area ratio. TP, MWD, and SWC were the main factors directly affecting the soil dyed area ratio, with path coefficients of 0.451, 0.346, and 0.291, respectively ($p < 0.001$). TP was itself affected by MWD and SOM, with path coefficients of 0.239 and 0.204, respectively ($p < 0.01$). MWD was in turn affected by SOM, RAD, and RLD, with path coefficients of 0.536 ($p < 0.001$), −0.325 ($p < 0.01$), and 0.213 ($p < 0.05$), respectively. SWC was affected by RAD, RLD, RMD, RSAD, and TP, with path coefficients of −0.424 ($p < 0.01$), 0.272, 0.064, 0.137, and 0.092 ($p < 0.05$), respectively (Figure 6A). The results of analysis of standard total, direct, and indirect effects showed that DC was indirectly affected by RAD, RLD, RMD, RSAD, and SOM and directly affected by MWD and TP. MWD also exerted an effect on SWC via TP. Therefore, TP, MWD, and SWC significantly affected preferential flow (Figures 6B–D).

4 Discussion

4.1 Effects of stump height on root and soil properties of *H. rhamnoides*

The responses of the growing properties of plants to stumping at different heights are complex (Bond and Midgley, 2001). The aboveground parts of a plant will undergo compensatory growth after destruction, which stimulates an increase in root biomass. Roots store abundant starch to provide nutrition for rapid recovery of the crown or foliage (Fang et al., 2006; Hamilton et al., 2013; Liu et al., 2023b). The present study analyzed the distributions of root and soil properties associated with different stump heights. The results showed that stumping significantly and directly promoted the root properties of *H. rhamnoides* and, as a consequence of these alterations to the roots, indirectly improved the properties of the understory soil.

RAD, RLD, RMD, and RSAD are all important indices for evaluation of the water and nutrient-absorbing abilities of plants (Florian et al., 2013; Cao et al., 2021). The results showed that, in each stump height condition, RLD, RMD, and RSAD all initially increased and then decreased with increasing soil depth. The values of the three indices all increased at a depth range of 0–20 cm, significantly decreased at 20–50 cm, and peaked at a depth of 10–20 cm. RLD, RMD, and RSAD were all significantly
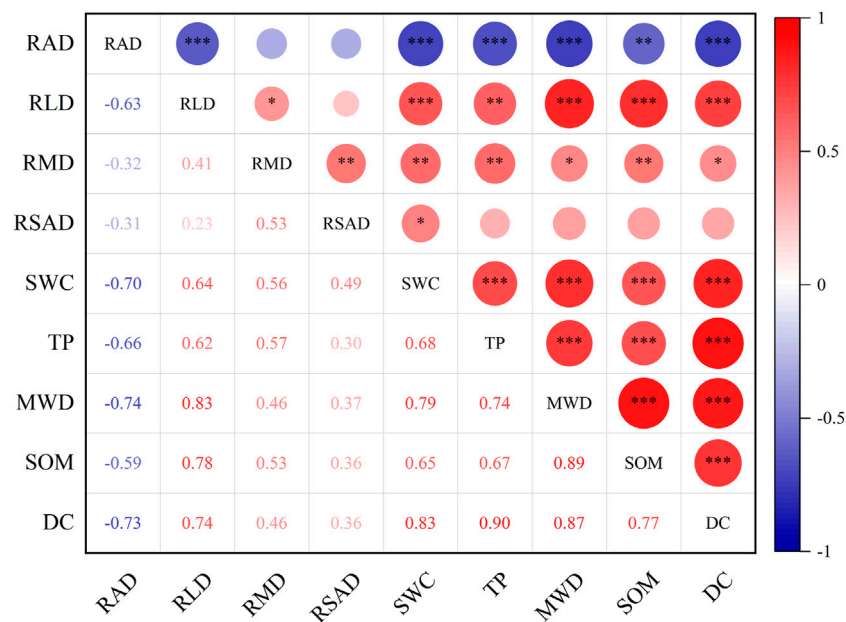
FIGURE 5
Pearson's correlation analysis of correlations between root and soil properties. RAD, root average diameter; RLD, root length density; RMD, root mass density; RSAD, root surface area density; SWC, soil moisture content; TP, total porosity; MWD, mean weight diameter; SOM, soil organic matter; DC, dye-tracing coverage. Blue and red indicate positive and negative correlations at significance levels of $*p < 0.05$, $**p < 0.01$, and $***p < 0.001$.

greater at a depth of 0–30 cm than at 30–50 cm (Figures 3B–D). The reason for the increase in RLD, RMD, and RSAD at a depth of 0–20 cm is that the roots of *H. rhamnoides* flourish the most in this layer in feldspathic sandstone areas. This type of root distribution is a shallow distribution. Furthermore, the horizontal roots are well developed, which can effectively improve the space-occupying ability of the roots and broaden the distributions of nutrients and moisture, both of which contribute to the effective use of soil moisture and nutrients. Moreover, in feldspathic sandstone areas with frequent wind-blown sand events, rich horizontal roots can better fix and support the entire plant compared to vertical roots (Yang et al., 2013; Yang et al., 2014; Liu et al., 2022). The reason the values of RLD, RMD, and RSAD peaked at a depth of 10–20 cm is that the roots of *H. rhamnoides* show the best response to stumping at this layer, and significant root growth improves the understory soil conditions, especially the soil moisture and nutrients, at the 10–20 cm depth. The improved soils further promote root development (Han et al., 2014; Liu et al., 2023a). Hence, the root properties all peaked at a depth of 10–20 cm regardless of stump height. The significant decrease in RLD, RMD, and RSAD at a depth of 30–50 cm can be explained by the fact that this layer contains more feldspathic sandstone, so it is very difficult for the roots to enter deep soils (Yang et al., 2013; Wang, 2018). Therefore, these indices decreased at this depth range (Figures 3B–D). RAD decreased with stump height because the surface roots are thick and contain many skeleton roots (Ong et al., 2002; Bardgett et al., 2014). The number of fine roots gradually increases with increasing soil depth, while the numbers of thick roots and skeleton roots decrease, leading to a decrease in RAD with increasing soil depth (Figure 3A).

The decrease in leaf area after stumping affected the allocation and transportation of metabolites and moisture between the aboveground and underground parts of the tree, thus causing changes in soil moisture content (Mooleki et al., 2016; Qi and Guo., 2020). The results showed that SWC first increased and then decreased with increasing soil depth with each of the different stump heights (Figure 4A). These results are essentially consistent with the soil moisture characteristics observed under conditions of deteriorating vegetation in typical feldspathic sandstone areas covered with loess (Ma, 2020; Zhang et al., 2020). This is mainly because soil moisture in this region mainly originates from natural precipitation, while supplementary moisture is essentially reserved in shallow soils and is hardly able to supplement deep soils. Moreover, most of the precipitation that falls on shallow soils is utilized by plants or evaporates from the ground. This is also one of the reasons why roots are distributed in the superficial layers (Yang et al., 2013). Since more soil macropores exist at depths of 0–10 cm (and due to the influence of air temperature), soil moisture in this layer is more likely to evaporate. Since the water-holding ability of the soil is lower at this layer than at depths of 10–20 cm (Wang, 2018), water content peaks at a vertical distance of 10–20 cm from the standard cluster (Figure 4A).

Soil TP, SOM, and MWD decreased significantly with increasing soil depth regardless of stump height, and were greater in surface soil than in deep soil. This occurs for two reasons: first, because the abundant plant litter on the topsoil of forest land decomposes into structurally diverse organic matter, which is the main source of organic matter in the soil (Liu and Lin, 2015; Niu et al., 2021). The second reason is that the metabolic activity of roots and secretions from them are also sources of soil organic matter. A significant

FIGURE 6
analysis of the effects of root and soil properties on DC. χ^2 = 11.838, χ^2/df = 0.789, p = 0.691 > 0.05, CFI = 1, RMSEA = 0.000, AIC = 71.838. R^2 indicates the proportion of variance explained by each variable. Single arrowheads indicate causality; double arrowheads indicate correlations; red indicates a positive effect and blue a negative effect; arrowhead thickness represents the value of the path coefficient. **(A)** Structural equation model; **(B)** standardized total effects; **(C)** standardized direct effects; **(D)** standardized indirect effects. All abbreviations are defined in Figure 4.

increase in soil organic matter and the metabolic activities of roots decreases soil bulk density, thus increasing TP and MWD (Wang et al., 2017; Cui et al., 2019; Wu et al., 2020) (Figures 4B–D).

RLD, RMD, RSAD, and soil property indices were all significantly higher under S1, S2, S3, and S4 than in condition CK, and all were maximized at a stump height of 15 cm (Figures 3B–D). This indicates that root development of *H. rhamnoides* improved after stumping, which can promote root branching ability. Thus, the roots of *H. rhamnoides* grew significantly, which improved their ability to occupy space underground and compete for nutrition, effectively promoting root and even plant growth. This process also exerted soil stabilization effects and increased TP and MWD. Root development can loosen and penetrate soils and greatly promotes the infiltration of soil moisture. Moreover, this development can effectively preserve precipitation and exerts water-holding and soil-consolidating effects. Meanwhile, the metabolic ability of roots was enhanced; in this process, the metabolic activity of roots and root exudates can improve SOM. Thus, favorable soil moisture conditions can promote root growth and enable benign interactional circulation (Zhao et al., 2008; Hamilton et al., 2013; Liu et al., 2022) (Figure 4). This compensatory recovery and growth were optimized at a stump height of 15 cm, while the beneficial effects decreased at stump heights >15 cm (Figures 3, 4). RAD was smaller after any stumping treatment than without stumping, which is attributable to the fact

that stumping improved the branching ability of the roots and increased the number of fine roots, thereby decreasing RAD (Figure 3A).

4.2 Effects of root and soil properties on preferential flow behavior

The distribution of dye and the morphological characteristics of soil preferential flow reflect the evolving status and changing laws of preferential flow (Edith Allaire et al., 2011; Tobella et al., 2014). In this study, the characteristics of the soil preferential flow index showed that preferential flow occurred in the understory soils of *H. rhamnoides* in feldspathic sandstone areas, with dye area ratio generally decreasing with increasing soil depth (Figure 2); this is consistent with the findings of other studies (Kan et al., 2019; Kan et al., 2020). This occurred because the lower soils were compact, the moisture exchange between pores and the matrix was weaker than in the surface layer, and water flow always manifested as diverse macroporous flow (Luo Z. T. et al., 2019). Compared to CK, conditions S1, S2, S3, and S4 were all associated with intensification of the development of soil preferential flow (Table 1; Figure 2), indicating that stumping contributed to soil moisture infiltration. The root morphological characteristics differed with different stump heights; this indicates that the

movement forms of soil moisture differed (Jiang et al., 2019). The ranking of stump height conditions according to the degree of development of soil preferential flow was S3>S2>S1>S4>CK. The preferential flow characteristics of conditions S2 and S3 differed significantly from those of CK, and DC, MaxD, Unifr, PF$_{fr}$, and LI were also better under S3 (Table 1).

This pattern occurred because stumping promotes root growth, while root development (including that of rotten roots) further contributes to the formation of macropores in soil, thus improving soil structure and bioactivity and creating favorable conditions for the generation of preferential flow (Guo et al., 2018; Luo Z. et al., 2019). The un-stumped *H. rhamnoides* were already 10 years old, and the roots and aboveground parts were already decayed. The underground parts contained the pores formed by roots and rotten roots; however, root growth had gradually declined (Yang et al., 2014; Cao et al., 2016). As more roots became rotten, the understory soil pores were gradually plugged, and the number of macropores and the level of moisture infiltration decreased, which further aggravated plant decay and reduced the soil's water-holding capacity (Tang et al., 2018; Liu et al., 2020; Wang et al., 2023). Thus, stumping can alter the root growing conditions, and the improved root metabolic ability further increases soil porosity and aggregation. Consequently, soil preferential flow was improved by stumping in the present study; as a consequence, moisture penetrated into the deep soil, which had the effect of reducing ground erosion and promoting development that favored water holding and soil solidification (Cui et al., 2019; Wu et al., 2020). In concordance with these findings, Huang et al. (2017) have also found that root morphological characteristics affect the infiltration of soil moisture. The promotion of root growth and development facilitates the formation of more stable macropores and promotes preferential flow (Tang et al., 2018; Wang et al., 2020).

Soil moisture infiltration is affected by both the physicochemical properties of the soil and root properties (Hao H. X. et al., 2020; Liu et al., 2020). In this study, RSAD was not correlated with DC ($p >$ 0.05). RAD was very strongly negatively correlated with DC ($p <$ 0.001), while RLD, SWC, TP, MWD, and SOM were all very strongly positively correlated with DC ($p <$ 0.001). The ratio of dyed area of the soil was strongly correlated with indices of soil physicochemical properties and root parameters (Figure 5). This indicates that improvement in root distribution and soil physicochemical properties will facilitate the formation of preferential flow, thereby inducing preferential flow. This result is consistent with existing reports on the factors influencing preferential flow characteristics during vegetation recovery (Zhao et al., 2011; Hu et al., 2019). SEM analysis showed that DC was directly affected by TP, MWD, and SWC, while TP, MWD, and SWC explained 89.1% of the soil dyed area ratio, with path coefficients of 0.451, 0.346, and 0.291, respectively ($p <$ 0.001) (Figure 6A). This finding can be attributed to the fact that total soil porosity and pore connectivity directly affect preferential flow path and intensity (Shein, 2010). High aggregate stability improves soil porosity and decreases the coverage of water flow channels by clay grains, which offer stable and excellent channels for preferential flow development (Ghestem et al., 2011; Hao H. X. et al., 2020). When the soil moisture content is low, the movement of the water held within the soil pores is inhibited and the maximum infiltration depth is shallow (Edwards et al., 1993); however, high soil moisture content is

unfavorable for lateral infiltration, leading to an increase in maximum infiltration depth. Moreover, higher soil moisture content supports deeper preferential flow, which makes the preferential flow trend particularly clear (Beven and Germann, 1982; Liu et al., 2020).

The results showed that roots and soil organic matter indirectly affected soil moisture infiltration (Figure 6). Organic matter can act as an adhesive agent to improve the cohesive strength of soil, promoting granule formation and thereby promoting the formation of water-stable aggregates and improving soil structures, which in turn indirectly affects preferential flow behaviors in the soil (Hao H. X. et al., 2020). Roots mainly affect soil properties through indirect effects on soil moisture infiltration (Zhao et al., 2011; Hu et al., 2019) (Figure 6). This effect can be attributed to two mechanisms. First, roots can form connective macropores or channels by intervening in the soil. In particular, the macropore networks formed from topsoil roots become major preferential flow channels (Bogner et al., 2013), contributing to the movement of soil water. Second, root secretions and the rotting of dead roots contribute to organic matter accumulation, which promotes the formation of water-stable aggregates and the stabilization of soil pores, thus increasing the richness of preferential flow routes (Zhang et al., 2016). This is consistent with the findings of another study (Zhang et al., 2017) that roots are mainly distributed in topsoil and can effectively improve physicochemical properties to induce the formation of preferential flow. In the present study, TP and MWD directly affected DC, while MWD indirectly affected DC by impacting TP, which affected SWC. These direct and indirect effects enhanced the promoting effects of TP, MWD, and SWC on preferential flow behaviors (Figure 6).

The roots of *H. rhamnoides* were significantly improved by stumping at different heights; the metabolic activity and the development of roots were increased. Moreover, RLD, RMD, and RSAD all significantly increased, and TP, MWD, SWC, and SOM improved due to soil stabilization by the roots, root metabolic activity, and root exudates. The root distribution and the improved physicochemical properties of the soil then significantly affected the degree of preferential flow development (Ghestem et al., 2011; Tobella et al., 2014; Hao H. X. et al., 2020; Wang et al., 2020; Liu et al., 2022). The results of this study clarify the mechanism of preferential flow formation, offering theoretical and scientific bases for studying the protection and recovery of water sources for vegetation.

5 Conclusion

The effects of stump height on root and soil properties for *H. rhamnoides* were discussed. After stumping, the associated root and soil properties were better than those associated with trees that had not undergone stumping, and the optimal stump height was 15 cm. Stumping stimulated a significant increase in root development and improved root metabolic activity; it also increased soil porosity, aggregate stability, soil moisture content, and soil organic matter content, and these favorable soil conditions in turn promoted the growth of further roots and plants. Additionally, the changes in these properties after stumping significantly affected the degree of preferential flow development. TP, MWD, and SWC were the

main factors influencing direct control of DC. RAD, RLD, RMD, RSAD, and SOM played indirect roles. MWD directly affected DC and also affected TP, thereby indirectly affecting SWC. Therefore, TP, MWD, and SWC all significantly affected preferential flow. These findings indicate that stumping at a height of 15 cm results in stronger infiltration and preferential flow and can effectively increase the transportation of preferential moisture and nutrients, which are essential for the supply of moisture in deep soils and the recovery and growth of *H. rhamnoides* in feldspathic sandstone areas.

Data availability statement

The original contributions presented in the study are included in the article/Supplementary Material; further inquiries can be directed to the corresponding author.

Author contributions

LL: conceptualization, methodology, writing–original draft, visualization, data curation, software, investigation, and formal analysis. XL: conceptualization, methodology, writing–original draft, visualization, data curation, software, investigation, and formal analysis. YG: conceptualization, methodology, writing–original draft, writing–review and editing, supervision, and project administration. WQ: conceptualization, writing–original draft, investigation, and formal analysis. YY: conceptualization, writing–original draft, writing–review and editing, supervision, and project administration. All authors read and approved the final manuscript.

Conflict of interest

The authors declare that the research was conducted in the absence of any commercial or financial relationships that could be construed as a potential conflict of interest.

Publisher's note

All claims expressed in this article are solely those of the authors and do not necessarily represent those of their affiliated organizations, or those of the publisher, the editors, and the reviewers. Any product that may be evaluated in this article, or claim that may be made by its manufacturer, is not guaranteed or endorsed by the publisher.

References

Allaire, S. E., van Bochove, E., Denault, J. T., Dadfar, H., Theriault, G., Charles, A., et al. (2011). Preferential pathways of phosphorus movement from agricultural land to water bodies in the Canadian great lakes basin: A predictive tool. *Can. J. Soil Sci.* 91, 361–374. doi:10.4141/cjss09121

Bardgett, R. D., Mommer, L., and De Vries, F. T. (2014). Going underground: Root traits as drivers of ecosystem processes. *Trends Ecol. Evol.* 29, 692–699. doi:10.1016/j.tree.2014.10.006

Beven, K., and Germann, P. (1982). Macropores and water flow in soils. *Water Resour. Res.* 18, 1311–1325. doi:10.1029/WR018i005p01311

Bogner, C., Trancon, Y. W. B., and Lange, H. (2013). Characterising flow patterns in soils by feature extraction and multiple consensus clustering. *Ecol. Inf.* 15, 44–52. doi:10.1016/j.ecoinf.2013.03.001

Bond, W. J., and Midgley, J. J. (2001). Ecology of sprouting in woody plants: The persistence niche. *Trends Ecol. Evol.* 16, 45–51. doi:10.1016/S0169-5347(00)02033-4

Cao, J. J., Wei, C., Adamowski, J. F., Biswas, A., Li, Y. M., Zhu, G. F., et al. (2021). On China's qinghai-Tibetan plateau, duration of grazing exclosure alters R: S ratio, root morphology and attending root biomass. *Soil Tillage Res.* 209, 104969. doi:10.1016/j.still.2021.104969

Cao, Z. L., Li, T. J., Li, G. Q., Liu, C. H., Gao, H. Y., Dai, G. H., et al. (2016). Modular growth and clonal propagation of *Hippophae rhamnoides* subsp *sinensis* in response to irrigation intensity. *J. For. Res.* 27, 1019–1028. doi:10.1007/s11676-016-0236-z

Cui, Z., Wu, G. L., Huang, Z., and Liu, Y. (2019). Fine roots determine soil infiltration potential than soil water content in semi-arid grassland soils. *J. Hydrol.* 578, 124023. doi:10.1016/j.jhydrol.2019.124023

Edwards, W. M., Shipitalo, M. J., Owens, L. B., and Dick, W. A. (1993). Factors affecting preferential flow of water and atrazine through earthworm burrows under continuous No-Till Corn. *J. Environ. Qual.* 22, 453–457. doi:10.2134/jeq1993.00472425002200030008x

Fang, X. W., Wang, X. Z., Li, H., Chen, K., and Wang, G. (2006). Responses of *Caragana korshinskii* to different aboveground shoot removal: Combining defence and tolerance strategies. *Ann. Bot.* 98, 203–211. doi:10.1093/aob/mcl088

Florian, F., Claire, J., and Pablo, C. (2013). Root and leaf functional trait relations in *poaceae* species: Implications of differing resource-acquisition strategies. *J. Plant Ecol.* 6, 211–219. doi:10.1093/jpe/rts034

Flury, M., Fluhler, H., Jury, W. A., and Leuenberger, J. (1994). Susceptibility of soils to preferential flow of water: A field study. *Water Resour. Res.* 30, 1945–1954. doi:10.1029/94WR00871

Ghestem, M., Sidle, R. C., and Stokes, A. (2011). The influence of plant root systems on subsurface flow: Implications for slope stability. *BioScience* 61, 869–879. doi:10.1525/bio.2011.61.11.6

Giambalvo, D., Amato, G., and Stringi, L. (2011). Effects of stubble height and cutting frequency on regrowth of Berseem clover in a Mediterranean semiarid environment. *Crop Sci.* 51, 1808–1814. doi:10.2135/cropsci2010.05.0271

Guan, Z. M., and Hao, C. Y. (2013). The fragile ecosystem types in arid and semi-arid region of China and their degradation causes. *Ecol. Econ.* 9, 158–162. (In Chinese).

Guo, L., Fan, B., Zhang, J., and Li, H. (2018). Occurrence of subsurface lateral flow in the Shale Hills Catchment indicated by a soil water mass balance method. *Eur. J. Soil Sci.* 69, 771–786. doi:10.1111/ejss.12701

Guo, L., Liu, Y., Wu, G. L., Huang, Z., Cui, Z., Cheng, Z., et al. (2019). Preferential water flow: Influence of alfalfa (*Medicago sativa* L.) decayed root channels on soil water infiltration. *J. Hydrol.* 578, 124019. doi:10.1016/j.jhydrol.2019.124019

Hamilton, S. A., Kallenbach, R. L., Bishop Hurley, G. J., and Roberts, C. A. (2013). Stubble height management changes the productivity of perennial ryegrass and tall fescue pastures. *Agron. J.* 105, 557–562. doi:10.2134/agronj2012.0293

Han, X., Sistla, S. A., Zhang, Y. H., Lu, X. T., and Han, X. G. (2014). Hierarchical responses of plant stoichiometry to nitrogen deposition and mowing in a temperate steppe. *Plant Soil* 382, 175–187. doi:10.1007/s11104-014-2154-1

Hao, H. X., Di, H. Y., Jiao, X., Wang, J. G., Guo, Z. L., and Shi, Z. (2020b). Fine roots benefit soil physical properties key to mitigate soil detachment capacity following the restoration of eroded land. *Plant Soil* 446, 487–501. doi:10.1007/s11104-019-04353-x

Hao, H. X., Wei, Y. J., Cao, D. N., Guo, Z. L., and Shi, Z. H. (2020a). Vegetation restoration and fine roots promote soil infiltrability in heavy-textured soils. *Soil Tillage Res.* 198, 104542. doi:10.1016/j.still.2019.104542

Hu, X., Li, X. Y., Wang, P., Liu, Y., Wu, X. C., Li, Z. C., et al. (2019). Influence of exclosure on CT-measured soil macropores and root architecture in a shrub-encroached grassland in northern China. *Soil Tillage Res.* 187, 21–30. doi:10.1016/j.still.2018.10.020

Huang, Z., Tian, F. P., Wu, G. L., Liu, Y., and Dang, Z. Q. (2017). Legume grass-lands promote precipitation infiltration better than gramineous grasslands in arid regions. *Land Degrad Dev.* 28, 309–316. doi:10.1002/ldr.2635

Jarvis, N. J. (2007). A review of non-equilibrium water flow and solute transport in soil macropores: Principles, controlling factors and consequences for water quality. *Eur. J. Soil Sci.* 58, 279–302. doi:10.1111/ejss.12973

Jiang, X. J., Chen, C., Zhu, X., Zakari, S., Singh, A. K., Zhang, W., et al. (2019). Use of dye infiltration experiments and HYDRUS-3D to interpret preferential flow in soil in a rubberbased agroforestry systems in Xishuangbanna, China. *Catena* 178, 120–131. doi:10.1016/j.catena.2019.03.015

Kan, X. Q., Cheng, J. H., and Hou, F. (2020). Response of preferential soil flow to different infiltration rates and vegetation types in the Karst region of southwest China. *Water* 12, 1778. doi:10.3390/w12061778

Kan, X. Q., Cheng, J. H., Hu, X. J., Zhu, F. F., and Li, M. (2019). Effects of grass and forests and the infiltration amount on preferential flow in Karst regions of China. *Water* 11, 1634. doi:10.3390/w11081634

Khan, M. R., Koneshloo, M., Knappett, P. S. K., Ahmed, K. M., Bostick, B. C., Mailloux, B. J., et al. (2016). Megacity pumping and preferential flow threaten groundwater quality. *Nat. Commun.* 7, 12833. doi:10.1038/ncomms12833

Langworthy, A. D., Rawnsley, R. P., Freeman, M. J., Corkrey, R., Harrison, M. T., Pembleton, K. G., et al. (2019). Effect of stubble-height management on crown temperature of perennial ryegrass, tall fescue and chicory. *Crop Pasture Sci.* 70, 183. doi:10.1071/CP18313

Liang, Z. S., Liu, H., Zhao, Y., Wang, Q., Wu, Z., Deng, L., et al. (2020). Effects of rainfall intensity, slope angle, and vegetation coverage on the erosion characteristics of Pisha sandstone slopes under simulated rainfall conditions. *Environ. Sci. Pollut. Res.* 27, 17458–17467. doi:10.1007/s11356-019-05348-y

Liu, H., and Lin, H. (2015). Frequency and control of subsurface preferential flow: From pedon to catchment scales. *Soil Sci. Soc. Am. J.* 79, 362–377. doi:10.2136/sssaj2014.08.0330

Liu, L., Guo, Y. F., Liu, X. Y., Yao, Y. F., and Qi, W. (2023a). Relationship between the roots of *Hippophae rhamnoides* at different stump heights and the root microenvironment in feldspathic sandstone areas. *Peerj* 11, e14819. doi:10.7717/peerj.14819

Liu, L., Guo, Y. F., Liu, X. Y., Yao, Y. F., and Qi, W. (2022). Stump height after regenerative cutting of sea-buckthorn (*Hippophae rhamnoides*) affects fine root architecture and rhizosphere soil stoichiometric properties. *Rhizosphere* 24, 100602. doi:10.1016/j.rhisph.2022.100602

Liu, L., Guo, Y. F., Liu, X. Y., Yao, Y. Y., and Qi, W. (2023b). Coordinated variation in root and leaf functional traits of *Hippophae rhamnoides* treated at different stump heights in feldspathic sandstone areas of Inner Mongolia. *Front. Plant Sci.* 14, 1104632. doi:10.3389/fpls.2023.1104632

Liu, W., Guo, Z., Jiang, B., Lu, F., Wang, H., Wang, D., et al. (2020). Improving wetland ecosystem health in China. *Ecol. Indic.* 113, 106184. doi:10.1016/j.ecolind.2020.106184

Liu, Y., Zhang, Y., Xie, L., Zhao, S., Dai, L., and Zhang, Z. (2021). Effect of soil characteristics on preferential flow of *Phragmites australis* community in Yellow River delta. *Ecol. Indic.* 125, 107486. doi:10.1016/j.ecolind.2021.107486

Luo, Z., Niu, J., Xie, B., Zhang, L., Chen, X., Berndtsson, R., et al. (2019b). Influence of root distribution on preferential flow in deciduous and coniferous forest soils. *Forests* 10, 986. doi:10.3390/f10110986

Luo, Z. T., Niu, J. Z., Zhang, L., Chen, X., Zhang, W., Xie, B., et al. (2019a). Roots-Enhanced preferential flows in deciduous and coniferous forest soils revealed by dual-Tracer experiments. *J. Environ. Qual.* 48, 136–146. doi:10.2134/jeq2018.03.0091

Ma, Z. H. (2020). *Characteristic and regulation of soil moisture under typical degraded vegetation in Loess covered Pisha sandstone area*. Xianyang, China: Northwest A and F University. (In Chinese).

Maier, F., van Meerveld, I., Greinwald, K., Gebauer, T., Lustenberger, F., Hartmann, A., et al. (2020). Effects of soil and vegetation development on surface hydrological properties of moraines in the Swiss Alps. *Catena* 187, 104353. doi:10.1016/j.catena.2019.104353

Mei, X., Zhu, Q., Ma, L., Zhang, D., Wang, Y., and Hao, W. (2018). Effect of stand origin and slope position on infiltration pattern and preferential flow on a loess hillslope. *Land Degrad. Dev.* 29, 1353–1365. doi:10.1002/ldr.2928

Mooleki, S. P., Gan, Y., Lemke, R. L., Zentner, R. P., and Hamel, C. (2016). Effect of green manure crops, termination method, stubble crops, and fallow on soil water, available N, and exchangeable P. *Can. J. Plant Sci.* 96, 867–886. doi:10.1139/cjps-2015-0336

Niu, H., Wu, H., Chen, K., Sun, J., Cao, M., and Luo, J. (2021). Effects of decapitated and root-pruned Sedum alfredii on the characterization of dissolved organic matter and enzymatic activity in rhizosphere soil during Cd phytoremediation. *J. Hazard. Mater.* 417, 125977. doi:10.1016/j.jhazmat.2021.125977

Ong, C. K., Raussen, T., Wajja-Musukwe, N., Wilson, J., Deans, J. D., Mulayta, J., et al. (2002). Tree-crop interactions: Manipulation of water use and root function. *Agric. Water Manag.* 53, 171–186. doi:10.1016/S0378-3774(01)00163-9

Qi, W., and Guo, Y. F. (2020). Study on the soil water content and physiological properties after stumping *Caragana korshinskii* at the farming-pastoral ecotone of Inner Mongolia. *Basic Clin. Pharmacol. Toxicol.* 126, 11.

Shao, W., Bogaard, T. A., Bakker, M., and Greco, R. (2015). Quantification of the influence of preferential flow on slope stability using a numerical modelling approach. *Hydrology Earth Syst. Sci.* 19, 2197–2212. doi:10.5194/hess-19-2197-2015

Shein, E. (2010). Soil hydrology: Stages of development, current state, and nearest prospects. *Eurasian Soil Sci-ence* 43, 158–167. doi:10.1134/S1064229310020055

Song, Y., Lu, Y., Guo, Z., Xu, X., Liu, T., Wang, J., et al. (2019). Variations in soil water content and evapotranspiration in relation to precipitation pulses within desert steppe in Inner Mongolia, China. *Water* 11, 198. doi:10.3390/w11020198

Sun, D., Yang, H., Guan, D. X., Yang, M., Wu, J., Yuan, F., et al. (2018). The effects of land use change on soil infiltration capacity in China: A meta-analysis. *Sci. Total Environ.* 626, 1394–1401. doi:10.1016/j.scitotenv.2018.01.104

Tang, B. Z., Jiao, J. Y., Yan, F. C., and Li, H. (2018). Variations in soil infiltration capacity after vegetation restoration in the hilly and gully regions of the Loess Plateau, China. *J. Soils Sediments* 19, 1456–1466. doi:10.1007/s11368-018-2121-1

Tobella, A. B., Reese, H., Almaw, A., Bayala, J., Malmer, A., Laudon, H., et al. (2014). The effect of trees on preferential flow and soil infiltrability in an agroforestry parkland in semiarid Burkina Faso. *Water Resour. Res.* 50, 3342–3354. doi:10.1002/2013WR015197

van Schaik, N. L. M. B. (2009). Spatial variability of infiltration patterns related to site characteristics in a semi-arid watershed. *Catena* 78, 36–47. doi:10.1016/j.catena.2009.02.017

Wang, D., Liu, C., Yang, Y. S., Liu, P. P., Hu, W., Song, H. Q., et al. (2023). Clipping decreases plant cover, litter mass, and water infiltration rate in soil across six plant community sites in a semiarid grassland. *Sci. Total Environ.* 861, 160692. doi:10.1016/j.scitotenv.2022.160692

Wang, F., Chen, H., Lian, J., Fu, Z., and Nie, Y. (2018). Preferential flow in different soil architectures of a small karst catchment. *Vadose Zone J.* 17, 1–10. doi:10.2136/vzj2018.05.0107

Wang, H. (2018). *Study on the root architecture characteristics of the seabuckthorn under different habitats in the Pisha sandstone area*. Hebei, China: Northwest University. (In Chinese).

Wang, R., Dong, Z., Zhou, Z., Wang, N., Xue, Z., and Cao, L. (2020). Effect of vegetation patchiness on the subsurface water distribution in abandoned farmland of the Loess Plateau, China. *Sci. Total Environ.* 746, 141416. doi:10.1016/j.scitotenv.2020.141416

Wang, T., Zhang, Z., Li, Z., and Li, P. (2017). Grazing management affects plant diversity and soil properties in a temperate steppe in northern China. *Catena* 158, 141–147. doi:10.1016/j.catena.2017.06.020

Weiler, M., and Fluhler, H. (2004). Inferring flow types from dye patterns in macroporous soils. *Geoderma* 120, 137–153. doi:10.1016/j.geoderma.2003.08.014

Wu, G. L., Liu, Y., Yang, Z., Cui, Z., Deng, L., Chang, X. F., et al. (2017). Root channels to indicate the increase in soil matrix water infiltration capacity of arid reclaimed mine soils. *J. Hydrology* 546, 133–139. doi:10.1016/j.jhydrol.2016.12.047

Wu, G. L., Lopez Vicente, M., Huang, Z., Cui, Z., and Liu, Y. (2020). Preferential water flow through decayed root channels enhances soil water infiltration: Evaluation in distinct vegetation types under semi-arid conditions. *Hydrol. Earth Syst. Sci. Discuss.* 266, 1–22. doi:10.5194/hess-2020-266

Yang, F. S., Bi, C. F., Cao, M. M., Li, H. E., Wang, X. H., and Wu, W. (2014). Simulation of sediment retention effects of the double seabuckthorn plant flexible dams in the Pisha Sandstone area of China. *Ecol. Eng.* 71, 21–31. doi:10.1016/j.ecoleng.2014.07.050

Yang, F. S., Cao, M. M., Li, H. E., Wang, X. H., and Bi, C. F. (2013). Simulation of sediment retention effects of the single seabuckthorn flexible dam in the Pisha Sandstone area. *Ecol. Eng.* 52, 228–237. doi:10.1016/j.ecoleng.2012.11.010

Yang, Z. P., Minggagud, H., Baoyin, T. G. T., and Li, F. Y. H. (2020). Plant production decreases whereas nutrients concentration increases in response to the decrease of mowing stubble height. *J. Environ. Manage* 253, 109745. doi:10.1016/j.jenvman.2019. 109745

Zhan, J., Lei, T., Qu, L., Zhang, M., Chen, P., Gao, X., et al. (2019). Method to quantitatively partition the temporal preferential flow and matrix infiltration in forest soil. *Geoderma* 347, 150–159. doi:10.1016/j.geoderma.2019.03.026

Zhang, C. B., Liu, Y. T., Jiang, J., and Li, D. R. (2020). Influence of soil moisture content on pullout properties of Hippophae rhamnoides Linn. roots. *J. Mt. Sci.* 17, 2816–2826. doi:10.1007/s11629-020-6072-9

Zhang, K., Xu, M. A., and Wang, Z. Y. (2009). Study on reforestation with seabuckthorn in the Pisha Sandstone area. *J. Hydro-environment Res.* 3, 77–84. doi:10.1016/j.jher.2009.06.001

Zhang, W. J., and Yuan, S. S. (2019). Characterizing preferential flow in landfilled municipal solid waste. *Waste Manag.* 84, 20–28. doi:10.1016/j.wasman.2018. 11.023

Zhang, Y. H., Niu, J. Z., Zhang, M. X., Xiao, Z. X., and Zhu, W. L. (2017). Interaction between plant roots and soil water flow in response to preferential flow paths in Northern China. *Land Degrad. Dev.* 28, 648–663. doi:10.1002/ldr.2592

Zhang, Y. H., Zhang, M. X., Niu, J. Z., and Zheng, H. J. (2016). The preferential flow of soil: A widespread phenomenon in pedological perspectives. *Eurasian Soil Sci.* 49, 661–672. doi:10.1134/S1064229316060120

Zhao, W., Chen, S. P., and Lin, G. H. (2008). Compensatory growth responses to clipping in *Leymus chinensis* (Poaceae) under nutrient addition and water deficiency conditions. *Plant Ecol.* 139, 85–99. doi:10.1007/s11258-007-9336-3

Zhao, Y., Peth, S., Reszkowska, A., Gan, L., Krümmelbein, J., Peng, X., et al. (2011). Response of soil moisture and temperature to grazing intensity in a Leymus chinensis steppe, Inner Mongolia. *Plant soil* 340, 89–102. doi:10.1007/s11104-010-0460-9

Zhu, P., Zhang, G., Wang, H., and Xing, S. (2020). Soil infiltration properties affected by typical plant communities on steep gully slopes on the Loess Plateau of China. *J. Hydrol.* 590, 125535. doi:10.1016/j.jhydrol.2020.125535